

Separation of magnetic fields in geophysical studies using a 2-D multi-resolution Wavelet analysis approach¹

Osman N. Ucan¹, Serhat Seker², A. Muhittin Albora³, and Atilla Ozmen¹

¹ Istanbul University, Engineering Faculty, Electrical & Electronics Department, 34850, Avcýlar, İstanbul, Turkey.
E-mail: uosman@istanbul.edu.tr; aozmen@istanbul.edu.tr

² Istanbul Technical University, Electrical & Electronics, Engineering Faculty, 80626 Maslak, İstanbul, Turkey.
E-mail: seker@elk.itu.edu.tr

³ Istanbul University, Engineering Faculty, Geophysics Department, 34850, Avcýlar, İstanbul, Turkey. E-mail: muhittin@istanbul.edu.tr

(Received 3 January 2000; accepted 22 February 2000)

Abstract: A 2-D Multi-Resolution Wavelet Analysis is applied to the magnetic field separation problem. The advantages of this method are that it does not introduce significant distortion to the shape of the original image and is not significantly affected by the overlapping power spectra of regional and residual fields. The proposed method has been tested by using a synthetic example and has yielded satisfactory results.

Keywords: Multi Resolution Analysis, Wavelet Transform, Magnetic Anomaly.

INTRODUCTION

Potential-Field maps usually contain a number of anomalies which are superposed upon each other. For instance, a magnetic map may be composed of regional, local, and micro-anomalies. In this case the determination of the causative sources boundaries suffers from the nearby source interference that yields misallocation (Grauch and Cordell, 1987). Since one type of anomaly often masks another, the need arises to separate the various anomalies from each other.

In our model, we investigate a two-dimensional magnetic structure as shown in Figure 1. Here the vertical component Z of the field can be expressed as (Telford *et al.* 1981),

$$Z = (\text{Vertical component of field due to } -m) - (\text{Vertical component of field due to } +m)$$

$$Z = kF_0 S \left\{ \left(\frac{1}{r_1^2} \right) \left(\frac{z}{r_1} \right) - \left(\frac{1}{r_2^2} \right) \left(\frac{z + L \sin \alpha}{r_2} \right) \right\} =$$

$$= kF_0 S \left\{ \left(\frac{z}{r_1^3} \right) - \left(\frac{z + L \sin \alpha}{r_2^3} \right) \right\} \quad (1)$$

k is susceptibility, F_0 is the Earth's total field and S is surface area. Since we have assumed that the rod is magnetized along its axis, these expression are valid only under one or both of the following conditions:

- the intrinsic field of the rod is very much larger than the external one;

- the rod is oriented along the field direction.

Since one type of anomaly often masks another, the need arises to separate the various anomalies from each other.

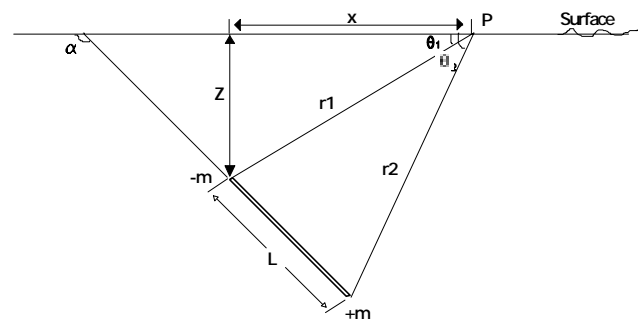


FIG. 1. Polarized magnetic dipole model.

Initial filtering operations to eliminate or attenuate unwanted field components include the radial weights methods (Griffin, 1989), least squares minimisation (Abdelrahman *et al.*, 1991), the Fast Fourier Transform methods (Bhattacharyya, 1976) and recursion filters (Vaclac *et al.*, 1992) and rational approximation techniques (Agarwal and Lal, 1971). A specific space-scale wavelet analysis, the Multi-Resolution Analysis (MRA), which allows decomposition of the signal with respect to a vast range of scales has been proposed by Fedi and Quarta 1998. Separation of regional and residual magnetic

¹ This work was supported by Istanbul University Research Fund. Project Number: 1247/050599.
© 2000 Balkan Geophysical Society, access <http://www.BalkanGeophySoc.org>

field data has been analysed by Yagou Li. and Douglas, (1998).

Magnetic anomaly separation can be affected by such wavelength filtering when magnetic response from the geologic feature of interest dominates one region of the observed magnetic field's power spectrum. Pawlowski *et al* (1990) have investigated a gravity anomaly separation method based on frequency-domain Wiener filtering. Hsu *et al* (1996) have presented a method for geological boundaries mapping from potential-field anomalies. Fedi *et al* (1999) have analysed upward continuation of potential field data to enhance the signal of deeper sources when shallower ones are present.

In this paper, 2-D Wavelet processing is applied to magnetic anomaly maps in real time. This modern and real time signal processing approach is tested using synthetic examples and produces satisfactory results. So 2-D Wavelet processing is thought to be a good alternative to classical potential field's anomaly separation methods.

WAVELET TRANSFORMS AND MULTI-RESOLUTION ANALYSIS

Magnetic data observed in geophysical surveys are the sum of magnetic fields produced by all underground sources. The targets for specific surveys are often small-scale structures buried at shallow depths. The response of these targets is often embedded in a regional field that arises from other sources usually larger or deeper than the targets or located further away. Good approximation removal of the regional field yields the residual field produced by the target sources. Interpretation and numerical modelling are carried out on the residual field data and the reliability of the interpretation depends to a great extent upon the success of the regional-residual separation.

Wavelets are functions that satisfy certain mathematical requirements and are used in representing data or other functions. In this manner, the Wavelet transform can be used to decompose a signal into different frequency components and then present each component with a resolution matched to its scale. In the signal analysis framework, the Wavelet transform of the time varying signal depends on the scale that is related to frequency and time. Hence, the Wavelets provide a tool for time-frequency localization.

As a result, the fundamental idea behind wavelets is to analyze according to scale. Therefore, wavelet algorithms can process data at different scales or resolutions. This concept of signal analysis is termed Multi-Resolution Analysis (MRA) and it makes the Wavelets intriguing and useful.

Wavelet Transforms

The wavelets, first mentioned by Haar in 1909, had a compact support which means that it vanishes outside of the finite interval, but Haar wavelets are not continuously differentiable. Later wavelets are considered with an effective algorithm for numerical image processing by an earlier discovered function that can vary in scale and can conserve energy when computing the functional energy (Gabor, 1946). Between 1960 and 1980, mathematicians such as Grossman and Morlet (1985) defined wavelets in the context of quantum physics. Mallat (1989) gave a boost to digital signal processing by inventing the pyramidal algorithms, and orthonormal wavelet bases. Later Daubechies (1990) used Mallat's work to construct a set of wavelet orthonormal basic functions that are the cornerstone of wavelet applications today.

The class of functions that present the wavelet transform are those that are square integrable on the real time. This class is denoted as $L^2(R)$.

$$f(x) \in L^2(R) \Rightarrow \int_{-\infty}^{+\infty} |f(x)|^2 dx < \infty \quad (2)$$

The set of functions that are generated in the wavelet analysis are obtained by dilating (scaling) and translating (time shifting) a single prototype function called the mother wavelet. The wavelet function $\psi(x) \in L^2(R)$ has two characteristic parameters called dilation (a) and translation (b), which vary continuously. A set of wavelet basis functions $\psi_{a,b}(x)$ may be given as

$$\psi_{a,b}(x) = \frac{1}{\sqrt{|a|}} \psi\left(\frac{x-b}{a}\right) \quad a, b \in R; a \neq 0 \quad (3)$$

Here, the translation parameter, " b ", controls the position of the wavelet in time. The "narrow" wavelet can access high frequency information, while the more dilated wavelet can access low frequency information. This means that the parameter " a " varies for different frequencies. The continuous wavelet transform is defined by

$$W_{a,b}(f) = \langle f, \psi_{a,b} \rangle = \int_{-\infty}^{+\infty} f(x) \psi_{a,b}(x) dx \quad (4)$$

The wavelet coefficients are given as the inner product of the function being transformed with each basis function.

Daubechies (1990) invented one of the most elegant families of wavelets. They are called Compactly Supported Orthonormal Wavelets, and are used in Discrete Wavelet Transform (DWT). In this approach, the scaling function is used to compute the ψ . The scaling function $\phi(x)$ and the corresponding wavelet $\psi(x)$ are defined by

$$\phi(x) = \sum_{k=0}^{N-1} c_k \phi(2x - k) \quad (5)$$

$$\psi(x) = \sum_{k=0}^{N-1} (-1)^k c_k \phi(2x + k - N + 1), \quad (6)$$

where N is an even number of wavelet coefficients c_k , $k = 0$ to $N-1$. The discrete presentation of an orthonormal compactly supported wavelet basis of $L^2(R)$ is formed by dilation and translation of signal function $\psi(x)$, called the wavelet function. It is assumed that the dilation parameters “ a ” and “ b ” take only the discrete values: $a = a_0^j$, $b = kb_0 a_0^j$, where $k, j \in Z$, $a_0 > 1$, and $b_0 > 0$. The wavelet function may be rewritten as

$$\psi_{j,k}(x) = a_0^{-j/2} \psi(a_0^{-j}x - kb_0) \quad (7)$$

and, the Discrete-Parameter Wavelet Transform (DPWT) is defined as:

$$\text{DPWT}(f) = \langle f, \psi_{j,k} \rangle = \int_{-\infty}^{+\infty} f(x) a_0^{-j/2} \psi(a_0^{-j}x - kb_0) dx \quad (8)$$

The choice between dilations and translations is made on the basis of the power of two, the so-called dyadic scales and positions, thus making the analysis efficient and accurate. In this case, the frequency axis is partitioned into bands by using the power of two for the scale parameter “ a ”. Considering samples at the dyadic values, one may get $b_0 = 1$ and $a_0 = 2$, and then the discrete wavelet transform becomes

$$\text{DPWT}(f) = \langle f, \psi_{j,k} \rangle = \int_{-\infty}^{+\infty} f(x) \{2^{-j/2} \psi(2^{-j}x - k)\} dx \quad (9)$$

Here, $\psi_{j,k}(x)$ is defined as

$$\psi_{j,k}(x) = 2^{-j/2} \psi(2^{-j}x - k), \quad j, k \in Z \quad (10)$$

Multi-resolution Analysis (MRA)

Mallat (1989) introduced an efficient algorithm to perform the DPWT known as the Multi-Resolution Analysis (MRA). It is well known in the signal processing area as the Two-Channel Sub-Band Coder. The MRA of $L^2(R)$ consists of successive approximations of the space V_j of $L^2(R)$. A scaling function $\phi(x) \in V_0$ exists such that

$$\phi_{j,k}(x) = 2^{-j/2} \phi(2^{-j}x - k); \quad j, k \in Z \quad (11)$$

For the scaling function $\phi(x) \in V_0 \subset V_1$, there is a sequence $\{h_k\}$,

$$\phi(x) = 2 \sum_k h_k \phi(2x - k) \quad (12)$$

This equation is known as the two-scale difference equation. Furthermore, let us define W_j as a comple-

mentary space of V_j in V_{j+1} , such that $V_{j+1} = V_j \oplus W_j$ and $\bigoplus_{j=-\infty}^{+\infty} W_j = L^2(R)$. Since the $\psi(x)$ is a wavelet and

it is also an element of V_0 , a sequence $\{g_k\}$ exists such that

$$\psi(x) = 2 \sum_k g_k \phi(2x - k) \quad (13)$$

It is concluded that the multiscale representation of a signal $f(x)$ may be achieved in different scales of the frequency domain by means of an orthogonal family of functions $\phi(x)$. Now, let us see how the function in V_j is computed. The projection of the signal $f(x) \in V_0$ on V_j defined by $P_v f^i(x)$ is given by

$$P_v f^i(x) = \sum_k c_{j,k} \phi_{j,k}(x) \quad (14)$$

Here, $c_{j,k} = \langle f, \phi_{j,k}(x) \rangle$. Similarly, the projection of the function $f(x)$ on the subspace W_j is also defined by

$$P_w f^j(x) = \sum_k d_{j,k} \psi_{j,k}(x) \quad (15)$$

where $d_{j,k} = \langle f, \psi_{j,k}(x) \rangle$. Because $V_j = V_{j-1} \oplus W_{j-1}$, the original function $f(x) \in V_0$ can be rewritten as

$$f(x) = \sum_k c_{j,k} \phi_{j,k}(x) + \sum_j \sum_k d_{j,k} \psi_{j,k}(x) \quad J > j_0 \quad (16)$$

The coefficients $c_{j,k}$ and $d_{j,k}$ are given by

$$c_{j-1,k} = \sqrt{2} \sum_i h_{i-2k} c_{j,k} \quad (17)$$

and

$$d_{j,k} = \sqrt{2} \sum_j g_{j-2k} c_{j,k} \quad (18)$$

The multiresolution representation is linked to Finite Impulse Response (FIR) filters. The scaling function ϕ and the wavelet ψ are obtained using the filter theory and consequently the coefficients are also defined by the last two equations. If at $x=t/2$, $F\{\phi(x)\}$ is considered and

$$\Phi(\omega) = H\left(\frac{\omega}{2}\right) \Phi\left(\frac{\omega}{2}\right) \quad (19)$$

As $\phi(0) \neq 0$, $H(0)=1$, this means that $H(\omega)$ is a low-pass filter. According to this result $\phi(t)$ is computed by the low-pass filter $H(\omega)$. The mother wavelet $\psi(t)$ is computed by defining the function $G(\omega)$ so that $H(\omega)G^*(\omega) + H(\omega + \pi)G^*(\omega + \pi) = 0$. Here, $H(\omega)$ and $G(\omega)$ are quadrature mirror filters for the MRA solution.

$$G(\omega) = -\exp(-j\omega) H^*(\omega + \pi). \quad (20)$$

Table I: Synthetic examples of polarized magnetic dipole data models.

Parameters	Dipole 1	Dipole 2	Dipole 3	Dipole 4	Dipole 5	Dipole 6	Dipole 7
(x,y) coordinate	0,0	7,-9	25,-20	15,15	-10,10	-30,30	-15,-10
D (deep)	8	4	3	4	5	3	3
L (along)	150	3	3	5	3	5	4
α (angle)	1	70	60	40	30	10	20

Table II: Synthetic examples of polarized magnetic dipole data models.

Parameters	Dipole 1	Dipole 2	Dipole 3	Dipole 4	Dipole 5	Dipole 6
(x,y) coordinate	0,0	17,-17	16,19	-18,17	-20,-18	0,-20
D (deep)	6	4	3	5	2	2
L (along)	15	4	2	3	1	3
α (angle)	5	90	60	30	47	20

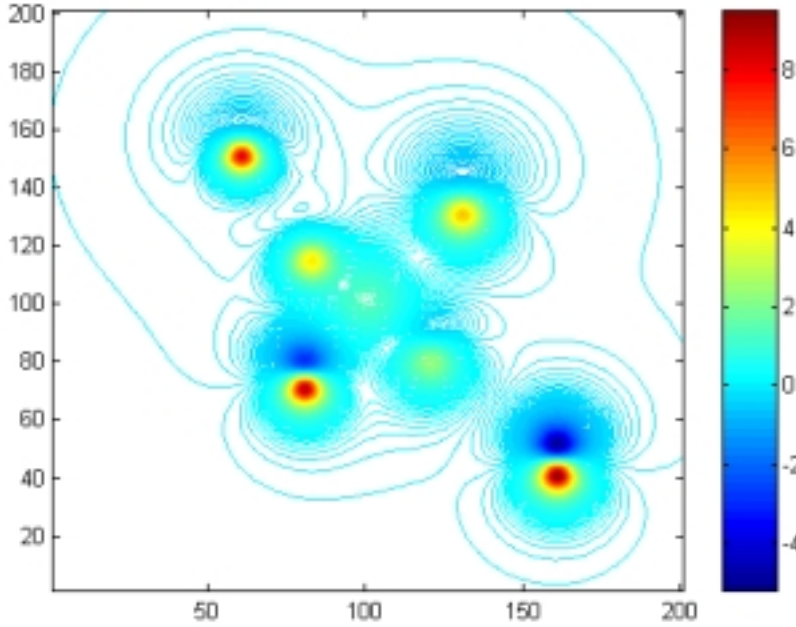


FIG. 2. Vertical magnetic field for different dipoles with properties given in Table I.

Substituting $H(0)=1$ and $H(\pi)=0$, it yields $G(0)=0$ and $G(\pi)=1$, respectively. This means that $G(\omega)$ is a high-pass filter. As a result, the MRA is a kind of Two-Channel Sub-Band Coder used in the high-pass and low-pass filters, from which the original signal can be reconstructed.

2-D Multi-Resolution Analysis

Since a major potential application of wavelets is in image processing, the 2-D wavelet transform is a necessity. The subject, however, is still at an evolving stage and in this section only the extension of 1-D wavelets to the 2-D case will be discussed. The idea is first to form a 1-D sequence from the 2-D image row sequences, do a 1-D MRA, restore the MRA outputs to

a 2-D format and repeat another MRA to the 1-D column sequences. The two steps of restoring to a 2-D sequence and forming a 1-D column sequence can be combined efficiently by appropriately selecting the proper points directly from the 1-D MRA outputs. After the 1-D row MRA, each low-pass and high-pass output goes through a 2-D restoration and 1-D column formation process and then moves on to another MRA. Let x_1 and x_2 , be the 2-D coordinates and $H = \text{low-pass}$, $G = \text{high-pass}$. Then the 2-D separable scaling function is

$$\phi^{(1)}(x_1, x_2) = \phi(x_1)\phi(x_2), \quad HH \quad (21)$$

the original signal can be reconstructed. Then 2-D separable wavelets are

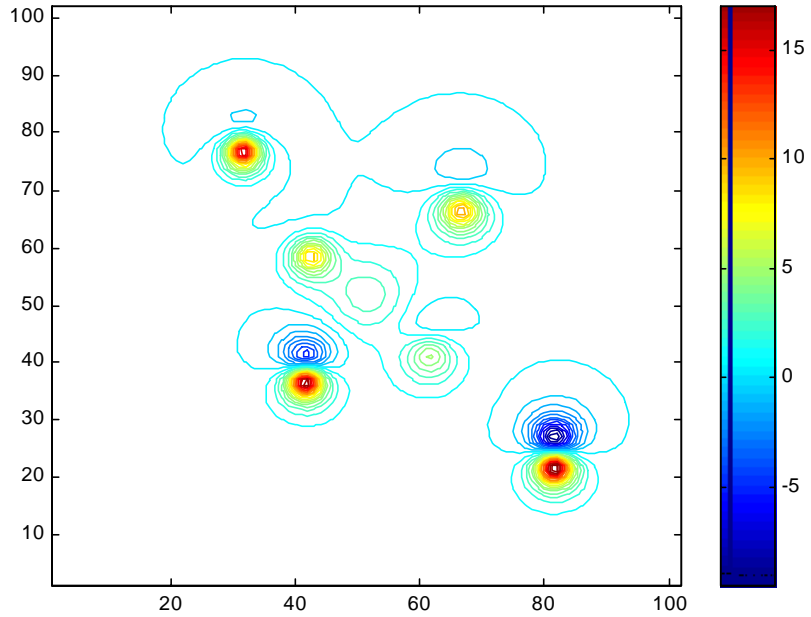


FIG. 3. Wavelet output of vertical magnetic field given in Figure 2.

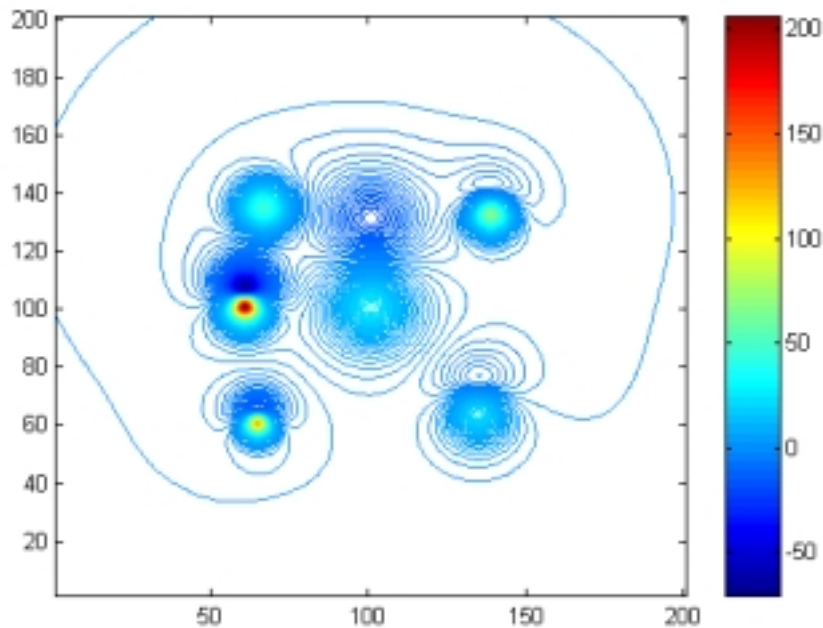


FIG. 4. Vertical magnetic field for different dipoles with properties given in Table II.

$$\psi^{(2)}(x_1, x_2) = \phi(x_1)\psi(x_2) , \quad HG \quad (22)$$

$$\psi^{(3)}(x_1, x_2) = \psi(x_1)\phi(x_2) , \quad GH \quad (23)$$

$$\psi^{(4)}(x_1, x_2) = \phi(x_1)\phi(x_2) , \quad GG \quad (24)$$

with the corresponding wavelet coefficients.

The scheme of separable 2-D processing, while being simple and using available 1-D filters, has disadvantages when compared to a genuine 2-D MRA with non-separable filters. The latter is more freely designed and can provide a better frequency and even a linear phase response. It also has non-rectangular sampling (Chan Y. T., 1996).

WAVELET APPLICATION ON A MAGNETIC ANOMALY MAP

The separation can also be performed by using a low-pass filter with a cut-off frequency determined by spectral analysis. Since the probability of properties and the neighbouring relations of the magnetic data is not taken into account in the classical approaches, disadvantages may arise from the overlapping of the residual and regional field spectra.

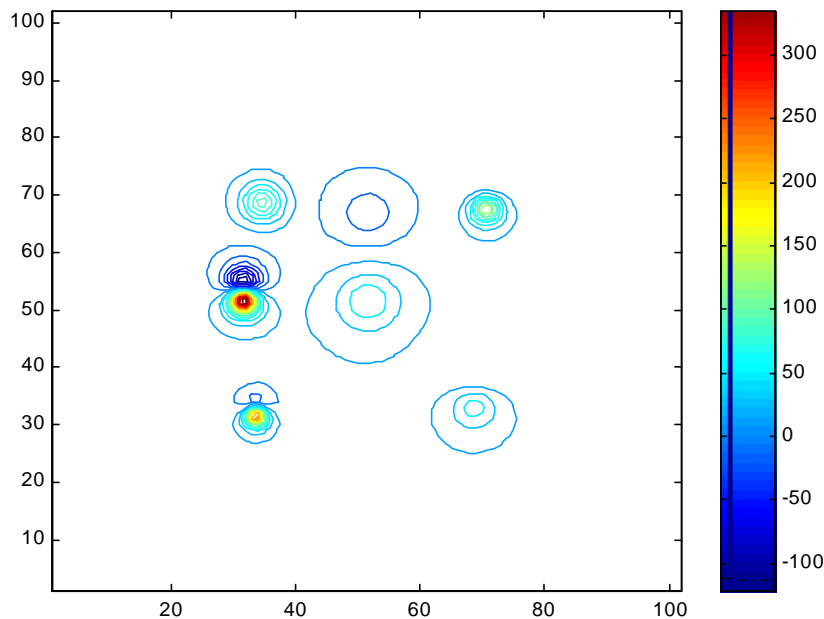


FIG. 5. Wavelet output of vertical magnetic field given in Figure 4.

We have tested our proposed approach on some synthetic data obtained by using equation 22-23. All the units used in the examples are normalized values. In the first example (Table I) seven dipoles structures are used (Figure 2). In the second example (Table II) six dipoles structures are used (Figure 4). At the wavelet output, the residual map is extracted satisfactorily as shown in Figure 3 and Figure 5.

CONCLUSION

In this paper, a 2-D Multi-Resolution Wavelet Analysis is used to solve a magnetic anomalies separation problem. The advantages of this method are that it does not introduce significant distortion to the shape of the original image and it is not affected significantly by the overlapping of the power spectra of regional and residual fields. The proposed method is tested by using synthetic examples and is considered to yield satisfactory results since at wavelet output the coordinates and properties of the dipoles can be easily observed.

ACKNOWLEDGEMENT

Thanks are due to the anonymous reviewers who helped improving the final version of this paper.

REFERENCES

- Abdelrahman, E. M., A. I., Bayoumi, H. M. El-Araby., 1991. A least-squares minimization approach to invert gravity data. *Geophysics*, **56**, 115-118.
- Agarwal, B. N. P., and Lal, L. T., 1971. Application of rational approximation in the calculation of the second derivative of the gravity field. *Geophysics*, **36**, 571-581.

- Bhattacharyya, B. K., and Navolio, M. E., 1976. A Fast Fourier Transform method for rapid computation of gravity and magnetic anomalies due to arbitrary bodies. *Geophysical Prospecting*, **20**, 633-649.
- Chan Y.T., 1996. *Wavelet Basics*. Kluwer Academic Publishers, USA.
- Daubechies, L., 1990. *The Wavelet Transform, Time-Frequency Localization and Signal Analysis*. *IEEE Trans. on Information Theory*, **36**.
- Fedi M., and Quarta T., 1998. Wavelet analysis for the regional-residual and local separation of potential field anomalies. *Geophysical Prospecting*, **46**, 507-525.
- Fedi M., Rapolla A. and Russo G., 1999. Upward continuation of scattered potential field data. *Geophysics*, **64**, 443-453.
- Gabor, D., 1946. *Theory of Communications*. *J.IEEE*, **93**, **3**, 429.
- Grauch, V. J. S., and Cordell, L., 1987. Limitations of determining density or magnetic boundaries from the horizontal gradient of gravity or pseudogravity data. *Geophysics*, **52**, 118-124.
- Griffin, W. P., 1989. Residual gravity in theory and practice. *Geophysics*, **14**, 39-56.
- Grossman, A., Morlet, 1985. *J., Mathematics and Physics*, **2**, L. Streit, Ed., World Scientific Publishing, Singapore.
- Mallat, S., 1989. *A Theory for Multiresolution Signal Decomposition of the Wavelet Representation*. *IEEE Trans. Pattern Anal. and Machine Intelligence*, **31**, 679-693.
- Pawlowski, R. S. and R. O. Hansen, 1990. Gravity anomaly separation by Wiener filtering. *Geophysics*, **55**, 539-548.
- Shu-Kun Hsu, Jean-Claude S., and Chuen-Tien S., 1996. High-resolution detection of geological boundaries from potential-field anomalies: An enhanced analytical signal technique. *Geophysics*, **61**, 373-386.
- Telford W. M., Geldart L. P., Sheriff R. E. and Keys D. A. 1981. *Applied Geophysics*. Cambridge University Press.
- Vaclac B., Jan H., and Karel S., 1992. Linear filters for solving the direct problem of potential fields. *Geophysics*, **57**, 1348-1351.
- Yagou Li., and Douglas W. O., 1998. Separation of regional and residual magnetic field data. *Geophysics*, **63**, 431-439.